JOURNAL OF MATERIALS SCIENCE 28 (1993) 5317–5324

Influence of vanadium on the static recrystallization of austenite in microalloyed steels

S. F. MEDINA
Metallurgical Research National Center (CENIM), Av. Gregorio del Amo 8, 28040 Madrid, Spain
J. E. MANCILLA
Autonomous University (UAP), Rio Sabinas 6109, 72570 Puebla, Mexico
C. A. HERNANDEZ
Autonomous National University (UNAM), Chemical Faculty (Ed. D), 04510 D.F., Mexico

Torsion tests were conducted to study the static recrystallization of three microalloyed steels manufactured by electroslag remelting (ESR) with different percentages of vanadium, 0.043%. 0.060% and 0.095%, respectively, and approximately equal percentages of the other alloy-forming elements. It was seen that, in contrast to niobium, dissolved vanadium has no influence on the activation energy. The influence only becomes notable when the precipitates start to form and the activation energy increases rapidly, thus inhibiting recrystallization. The critical temperature at which inhibition commences was measured as a function of the vanadium content and the deformation performed, and in all cases it was lower than the dissolution temperature deduced from the solubility products for nitrides, mainly because the testing conditions lacked thermodynamic equilibrium. Finally, a comparison was made of the microstructures obtained in two commercial steels, namely a C–Mn type steel and a vanadium microalloyed steel. Both were subjected to the same cycle of successive deformations, whose temperatures were lower than the critical temperature. After the last deformation, a much harder austenite was obtained in the microalloyed steel than in the C–Mn steel.

1. Introduction

Several authors have studied the static recrystallization of vanadium microalloyed steels when these are deformed in the austenitic phase. However, these studies have only been partial, for example at a certain temperature, deformation or chemical composition, and none has measured the activation energy of these steels.

In most metals, the statically recrystallized fraction follows Avrami's law, given by

$$X_a = 1 - \exp\left[(-\ln 2)\left(\frac{t}{t_{0.5}}\right)^n\right] \quad (1)$$

where $t_{0.5}$ is the time for the volumetric fraction of 0.5. The expression most widely used for this parameter is

$$t_{0.5} = A\varepsilon^p \dot{\varepsilon}^q D^s \exp\frac{Q}{RT} \quad (2)$$

where ε is the true strain, $\dot{\varepsilon}$ the strain rate, Q the activation energy, T the absolute temperature, $R = 8.138\ \mathrm{J\,mol^{-1}\,K^{-1}}$ and D the austenitic grain size.

It should be pointed out that the activation energy, Q, is the parameter most sensitive to chemical composition. In accordance with Equation 2, to calculate its value the recrystallized fraction must first be measured as a function of time and at different temperatures and, since this study involved microalloyed steels, for at least two strains, because strain influences the starting temperature of induced precipitation, below which the activation energy ceases to be constant and begins to increase drastically.

Several studies [1–5] give expressions for parameter $t_{0.5}$ where the activation energy has different values depending on whether the steels are C–Mn or Nb microalloyed, but do not consider Ti or V microalloyed steels.

Other authors [6, 7] have measured the recrystallized fraction of a V microalloyed steel and then compared their results with C–Mn steels and Nb microalloyed steels. Likewise, other results [8, 9] demonstrate that the vanadium percentage, and also the nitrogen percentage, have a slight influence on the recrystallized fraction.

In a recent publication [10], the following expression was given for the activation energy:

$$Q = 83600 + 978000\frac{(\mathrm{Mn} + \mathrm{Si})^{0.537}}{C^{1.269}} + 1728.7\,(\mathrm{Mo})^{0.704} + 4952 \times 10^{-5}\,(\mathrm{Ti})^{3.663} + 259.6\,(\mathrm{Nb})^{1.256} \quad (3)$$

0022–2461

where Q is given in $J\,mol^{-1}$ and the contents of the elements in wt % $\times 10^3$.

Equation 3 establishes that Q is a function of the chemical composition of the steel, and most of the alloying and microalloyng elements, such as C, Si, Mn, Mo, Ti and Nb, have been taken into account. Except for dissolved carbon, all the other elements increase the activation energy, and Nb delays recrystallization the most, both in dissolved and precipitate form. The accuracy of this equation has been verified in C–Mn steels, and Ti and Nb microalloyed steels, with carbon contents of over 0.045 wt %. In the case of Nb microalloyed steels, the critical temperature at which recrystallization inhibition starts must be considered, because below this temperature the activation energy increases considerably, signifying a progressive action of the recrystallization inhibition. Consequently, a term which takes this effect into account [10] must be added to the second member of Equation 3.

As will be seen later, V microalloyed steels react to static recrystallization in a different way to Ti and Nb microalloyed steels, not just because of the precipitation, which occurs at lower temperatures, but also because of the influence of the dissolved V on the activation energy. The quantitative measuring of the activation energy of these steels has an important application in forming processes, especially rolling, because it indicates the range of temperatures in which the deformed austenite may recrystallize after a rolling pass. It also accurately indicates the temperature below which the austenite recrystallizes only partially, and then starts to harden increasingly as the deformation temperature drops.

This paper presents a study of the influence of the vanadium percentage on the recrystallized fraction, measured at different temperatures and strains. The recrystallized fraction was measured by the double deformation technique, and the back extrapolation method [6] was chosen. It was seen that by employng this method, the softened fraction and the recrystallized fraction are approximately equal [4]. These results were used to calculate the activation energy in the steels and to measure its possible dependence on the vanadium percentage, both in dissolved and precipitate form, as well as to find the temperatures at which recrystallization starts to be inhibited.

As an application of the recrystallization study, we will show the microstructures of two steels, C–Mn and V microalloyed, obtained at the end of a series of successive torsional deformations which simulate the deformations of a finishing mill.

In accordance with the criterion of Von Mises, consideration was given to the very well-known equations [11–13] used in the transformation of the torsion magnitudes, given by the number of turns and the torque, in true strain and stress, respectively, as well as the equivalence with the rolling magnitudes.

2. Experimental procedure

The steels used to study the influence of vanadium on static recrystallization were manufactured by electroslag remelting (ESR), in a unit capable of producing 30 kg ingots. This technique avoids macrosegregation, both in alloying elements and impurities, and there is considerably less microsegregation, these defects being present in conventional ingots and continuous casting billets. In this way, the resulting specimens offer greater guarantees of accuracy.

TABLE I Chemical composition of steel (wt %) and critical temperature A_{r3}

Steel	C	Si	Mn	V	N (p.p.m.)	A_{r3}^{a} (°C)
V1	0.115	0.242	1.100	0.043	105	763
V2	0.125	0.241	1.050	0.060	123	762
V3	0.113	0.226	1.030	0.095	144	762
E1	0.192	0.287	1.290	—	—	760
VE2	0.120	0.362	1.420	0.040	95	765

[a] Cooling rate = 1 °C s^{-1}.

The other two steels used to establish a comparison of the microstructures that would be obtained from a hot rolling mill were commercial steels from continuous casting, C–Mn and V microalloyed steels, respectively. Their compositions are shown in Table I.

The torsion specimens, with a working surface 50 mm long and 6 mm in diameter, were austenized at 1230 °C for 10 min for the ESR-manufactured steels. Then the temperature was reduced to the testing temperature for approximately 2 min, long enough to stabilize at this temperature. The specimens were heated by induction, protected by a current of argon, and the temperature was monitored with a previously calibrated optical pyrometer.

To ensure that the testing temperatures corresponded to the austenitic phase, the critical transformation temperatures were measured by dilatometry. The values are given in Table I.

The recrystallized fraction in steels V1, V2 and V3 was measured at temperatures of 1100 °C, 1000 °C, 900 °C and 850 °C, a strain rate of 3.63 s^{-1} and strains of 0.20 and 0.35.

A finishing mill was simulated in the torsion machine with commercial steels E1 and VE2, at an austenization temperature of 1075 °C for 12 min. The specimens were quenched at the end of the last pass to obtain the microstructures that show the state of the austenite at that instant. The microstructures were also obtained after cooling at a rate of 3.5 °C s^{-1}, measured between 780 °C and 500 °C.

3. Results

First, the austenitic grain size of steels V1, V2 and V3 was measured at the austenization temperature (1230 °C; 10 min), which was calculated as the mean of the values obtained by linear intersection in the observation of 20 fields of the quenched microstructure. Similar values were obtained for the three steels: 172 μm, 167 μm and 165 μm, respectively (Table II).

The recrystallized fraction for each temperature and strain was measured as a function of time, and where total recrystallization occurred the resultant curves were plotted by regression with Equation 1.

Fig. 1 shows the recrystallized fraction of steel VI for a strain of 0.20 and at temperatures of 1100 °C, 1000 °C, 900 °C and 850 °C, respectively. Recrystallization was inhibited considerably at 850 °C. Fig. 2 refers to a strain of 0.35 and in this case no inhibition was observed at 850 °C, total recrystallization having occurred.

TABLE II Austenitic grain size (D), experimental (Q) and calculated (Q_c) activation energy according to Equation (3) and recrystallization critical temperature (T_c)

Steel	D (μm)	Q (kJ mol^{-1})	Q_c (kJ mol^{-1})	T_c (°C)[a]
V1	172	200	197	888 (0.20)
				855 (0.35)
V2	167	183	184	908 (0.20)
				887 (0.35)
V3	165	197	198	964 (0.20)
				908 (0.35)

[a] The number in parentheses is the strain.

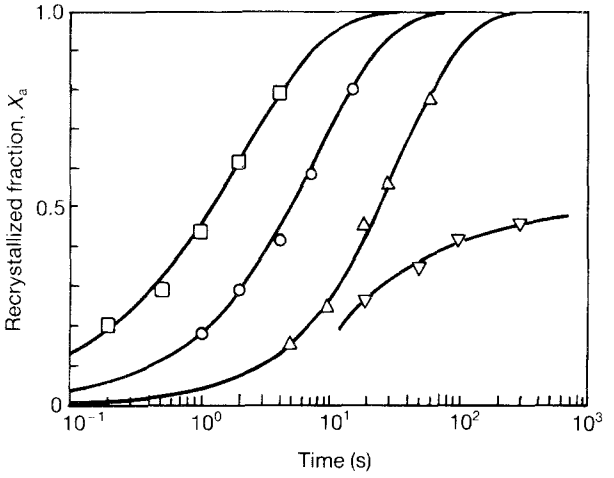

Figure 1 Recrystallized fraction plotted against time. Steel V1. $\varepsilon = 0.20$; $\dot{\varepsilon} = 3.62\,s^{-1}$ (□ = 1100 °C, ○ = 1000 °C, △ = 900 °C, ▽ = 850 °C).

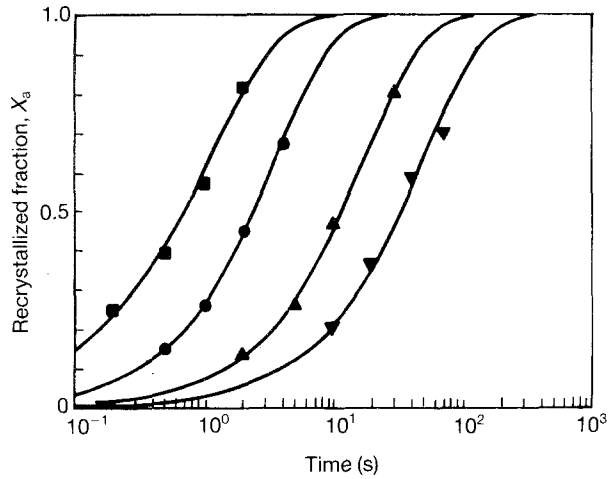

Figure 2 Recrystallized fraction plotted against time. Steel V1. $\varepsilon = 0.35$; $\dot{\varepsilon} = 3.62\,s^{-1}$ (■ = 1100 °C, ● = 1000 °C, ▲ = 900 °C, ▼ = 850 °C).

Figs 3 and 4 show the results obtained for steel V2 at strains of 0.20 and 0.35, respectively. A high degree of inhibition is observed in both cases.

Figs 5 and 6 refer to steel V3. A considerable inhibition of the recrystallization is seen to have occurred at

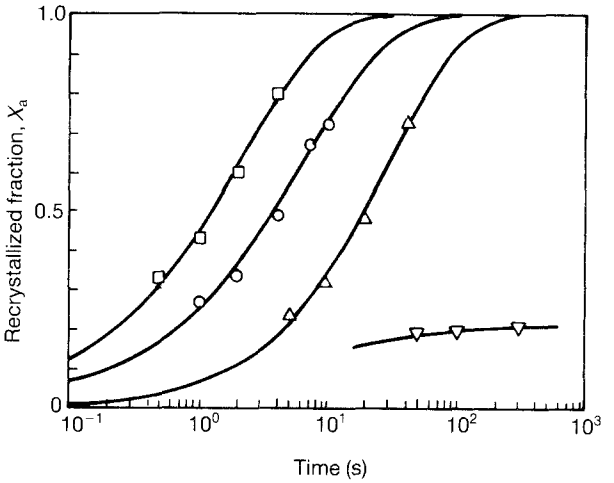

Figure 3 Recrystallized fraction plotted against time. Steel V2. $\varepsilon = 0.20$; $\dot{\varepsilon} = 3.62\ s^{-1}$ (□ = 1100 °C, ○ = 1000 °C, △ = 900 °C, ▽ = 850 °C).

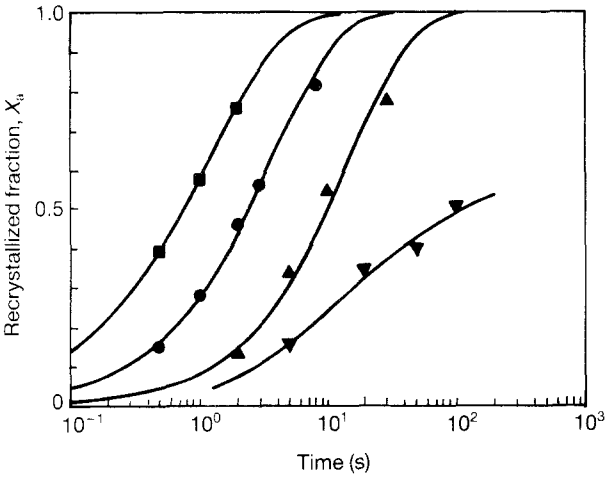

Figure 4 Recrystallized fraction plotted against time. Steel V2. $\varepsilon = 0.35$; $\dot{\varepsilon} = 3.62\,s^{-1}$ (■ = 1100 °C, ● = 1000 °C, ▲ = 900 °C, ▼ = 850 °C).

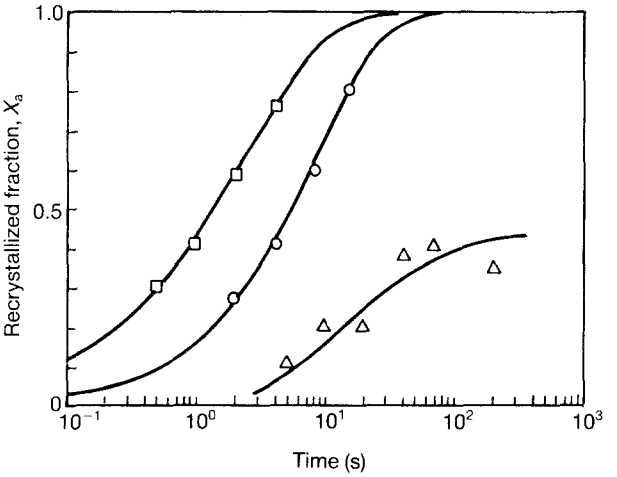

Figure 5 Recrystallized fraction plotted against time. Steel V3. $\varepsilon = 0.20$; $\dot{\varepsilon} = 3.62\ s^{-1}$ (□ = 1100 °C, ○ = 1000 °C, △ = 900 °C).

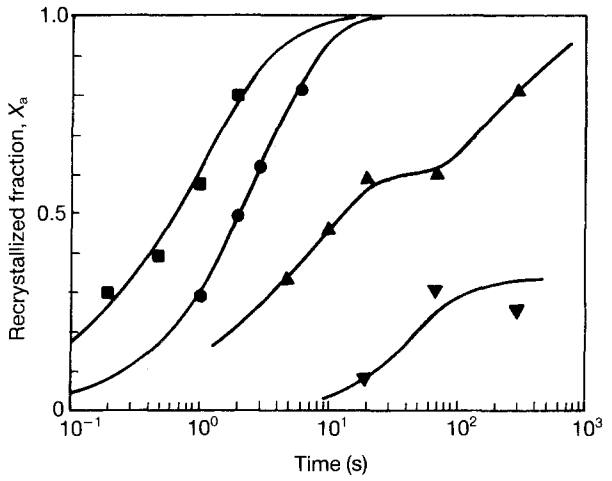

Figure 6 Recrystallized fraction plotted against time. Steel V3. $\varepsilon = 0.35$; $\dot{\varepsilon} = 3.62\,s^{-1}$ (■ = 1100 °C, ● = 1000 °C, ▲ = 900 °C, ▼ = 850 °C).

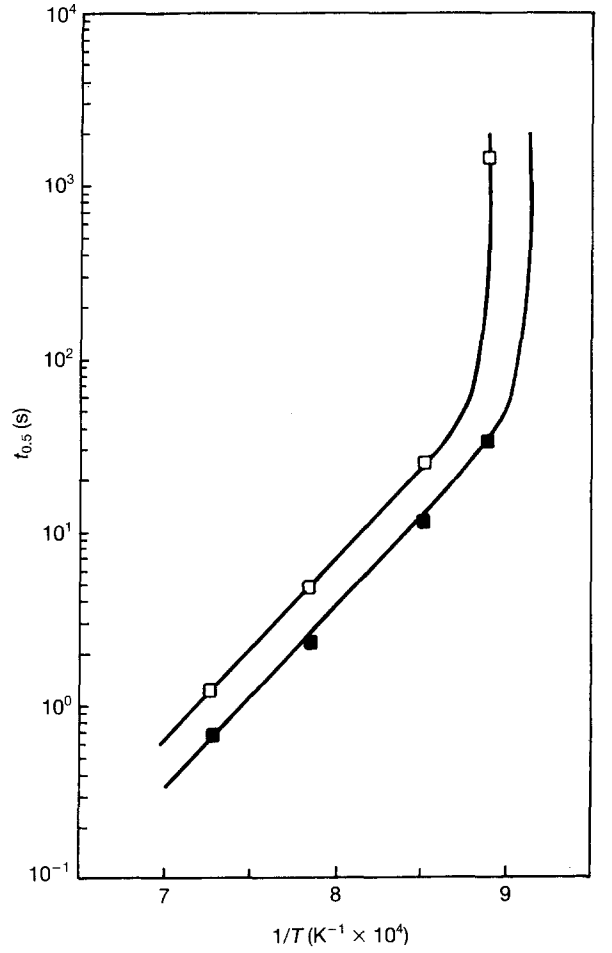

Figure 7 Parameter $t_{0.5}$ plotted against $1/T$. Steel V1. (□ $\varepsilon = 0.20$; ■ $\varepsilon = 0.35$).

higher temperatures than in the previous cases. Specifically, a high level of inhibition is observed at 900 °C with a strain of 0.20, and a low level with a strain of 0.35.

These results demonstrate that the temperature at which recrystallization starts to be inhibited is not only a function of the percentage of V, but also of the strain.

The activation energy was measured taking $\ln(t_{0.5})$ as a function of $1/T$, the slope being equal to Q/R. Figs 7–9 show the graphs for steels V1, V2 and V3, respectively, and the activation energy is constant to a certain temperature, below which it rises increasingly. Given that the activation energy is independent of the strain when the microalloying element is dissolved, the same parallelism criterion was adopted in plotting the curvilinear part. The activation energy was calculated for the interval of temperatures in which it is constant and at other points of the curvilinear part. Ln Q was plotted versus $1/T$, giving the graphs of Figs 10–12, which correspond to steels V1, V2 and V3, respectively, and the recrystallization critical temperature will be given by the intersection of the horizontal line with the sloping line.

In addition to the austenitic grain size, Table II shows the experimental activation energy for each steel in the temperature range in which it is constant ($T > T_c$), the activation energy calculated according to Equation 3 and the recrystallization critical temperature (T_c).

Although the testing conditions are not at thermodynamic equilibrium, because of the strain induced precipitation and the relatively quick cooling from the austenization temperature to the testing temperature, it is interesting to know what relationship exists between the dissolution temperature deduced from the solubility products for nitrides and carbides and the

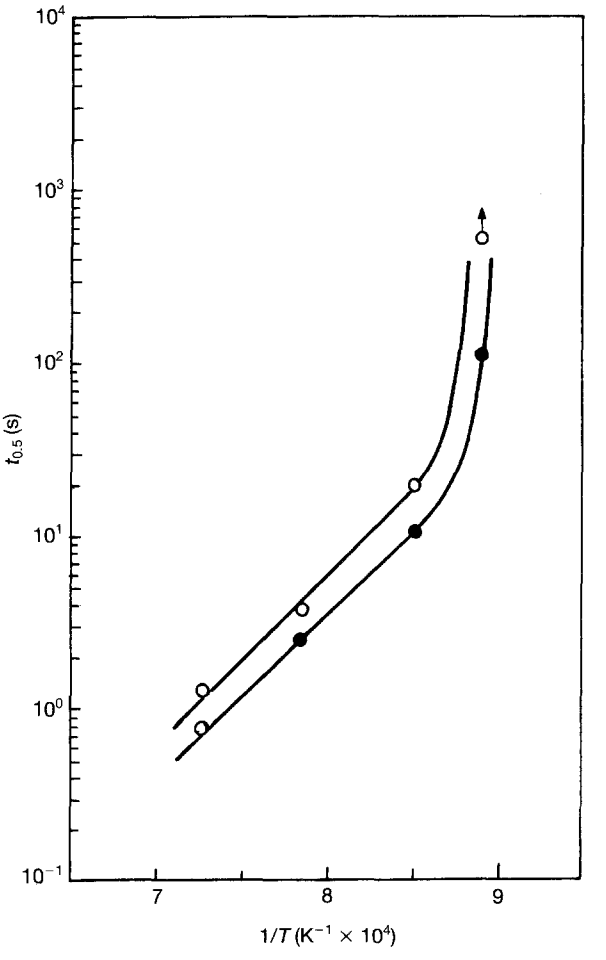

Figure 8 Parameter $t_{0.5}$ plotted against $1/T$. Steel V2. (○ $\varepsilon = 0.20$; ● $\varepsilon = 0.35$).

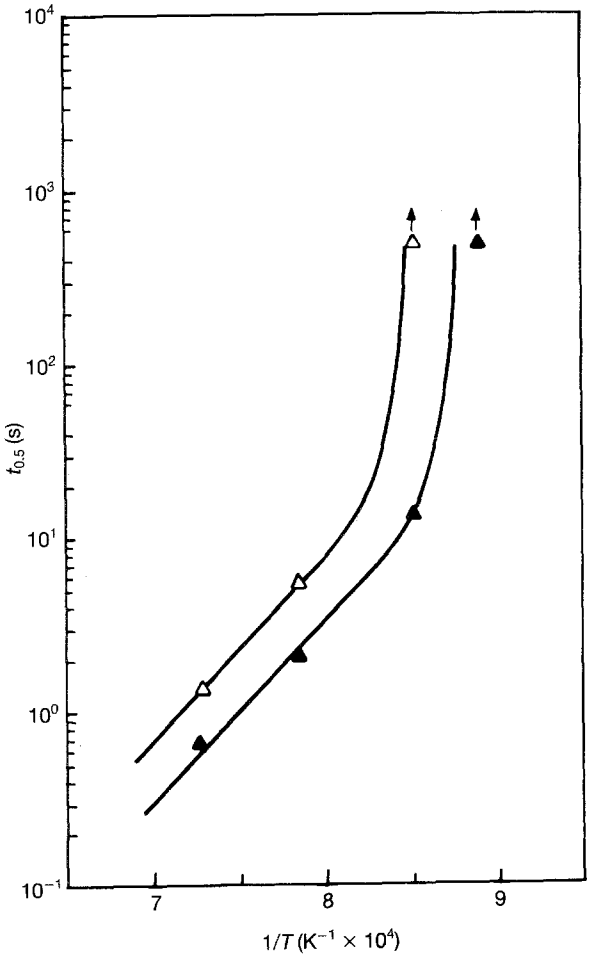

Figure 9 Parameter $t_{0.5}$ plotted against $1/T$. Steel V3. (△ $\varepsilon = 0.20$; ▲ $\varepsilon = 0.35$).

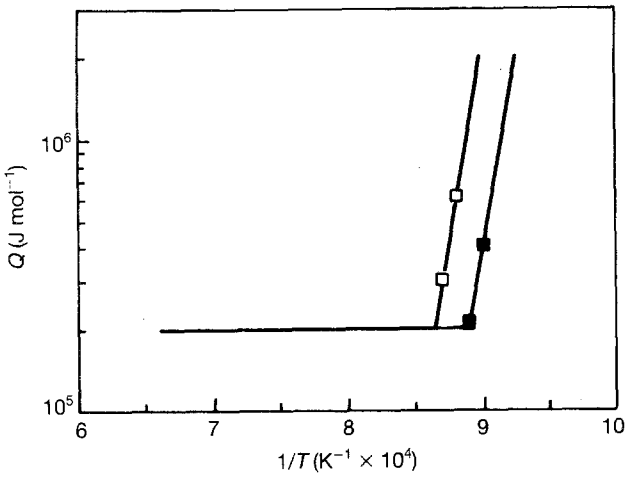

Figure 10 Activation energy plotted against $1/T$. Steel V1. (□ $\varepsilon = 0.20$; ■ $\varepsilon = 0.35$).

experimentally measured recrystallization critical temperatures. For this purpose, the following expressions were taken from [14]:

$$\log[N][V] = -\frac{8700}{T} + 3.63 \quad (4)$$

$$\log[C][V] = -\frac{9500}{T} + 6.72 \quad (5)$$

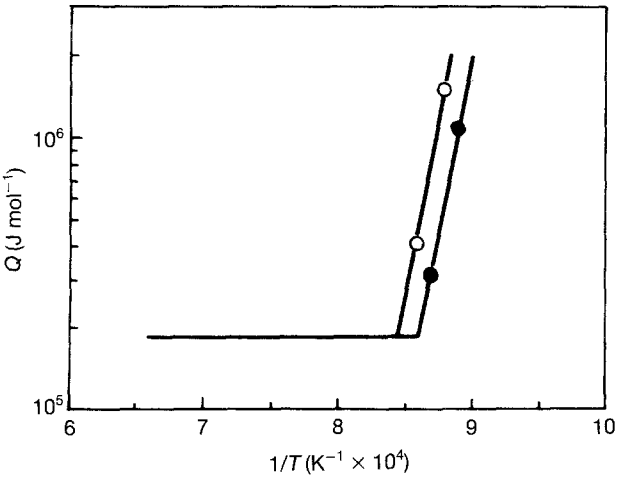

Figure 11 Activation energy plotted against $1/T$. Steel V2. (○ $\varepsilon = 0.20$; ● $\varepsilon = 0.35$).

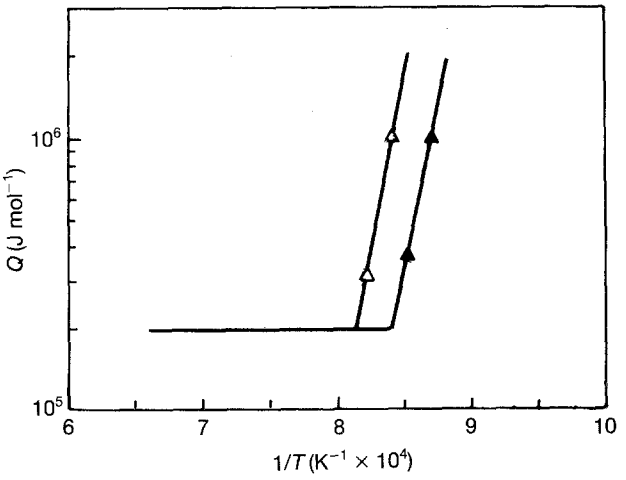

Figure 12 Activation energy plotted against $1/T$. Steel V3. (△ $\varepsilon = 0.20$; ▲ $\varepsilon = 0.35$).

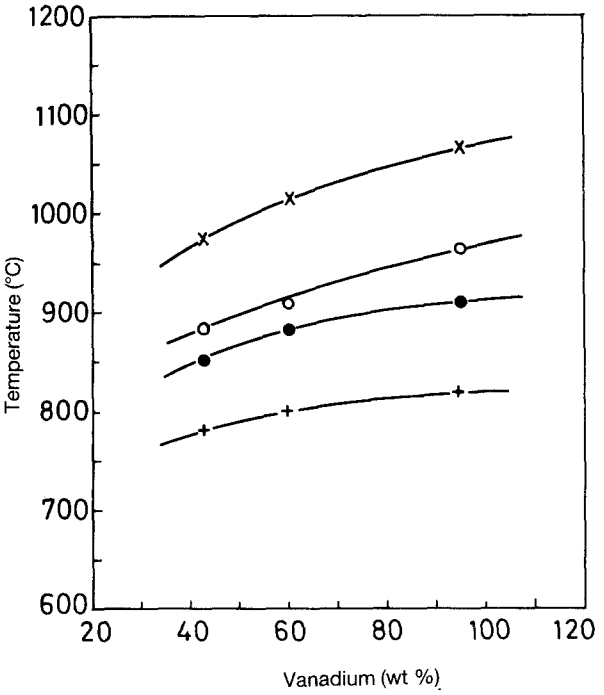

Figure 13 Dissolution temperature calculated according to Equations (4) and (5) and recrystallization critical temperature (T_c) against V wt %. [× NV; + CV; ○ T_c ($\varepsilon = 0.20$); ● T_c ($\varepsilon = 0.35$)].

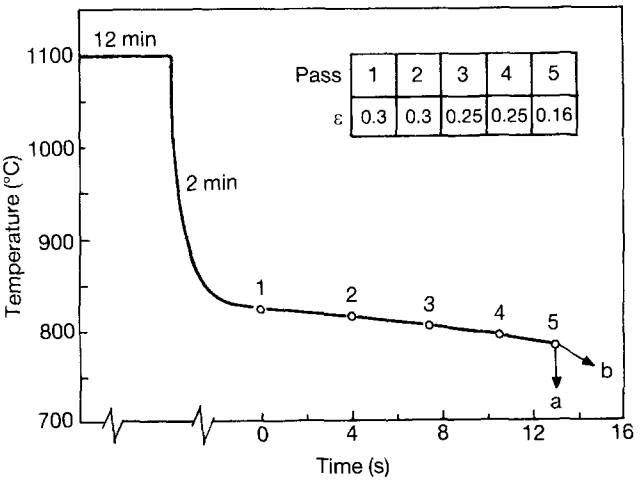

Figure 14 Torsion simulation schedule of finishing mill. (a) quenched; (b) cooling rate = 3.5 °C s^{-1}.

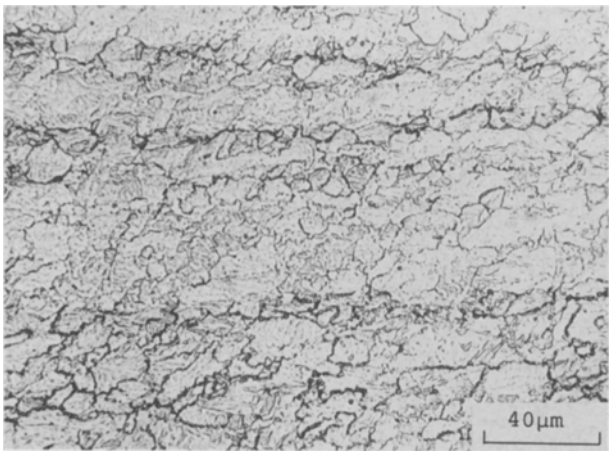

Figure 15 Effect of total finishing mill deformation on the austenite microstructure. Steel E1.

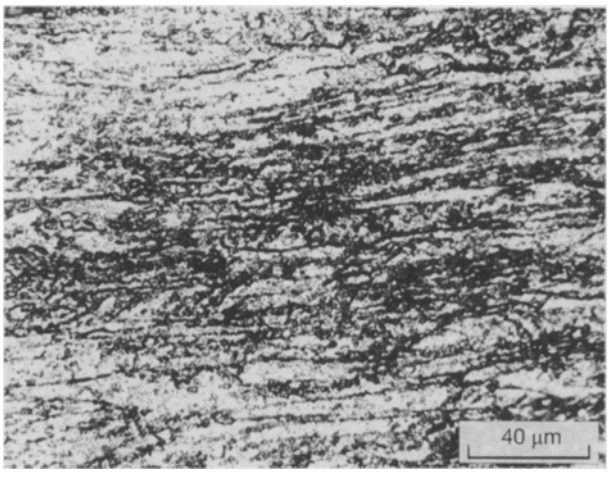

Figure 16 Effect of total finishing mill deformation on the austenite microstructure. Steel VE2.

and Fig. 13 shows the dissolution temperatures, T_s, that were calculated and the critical temperatures, T_c, as a function of the vanadium weight percentage.

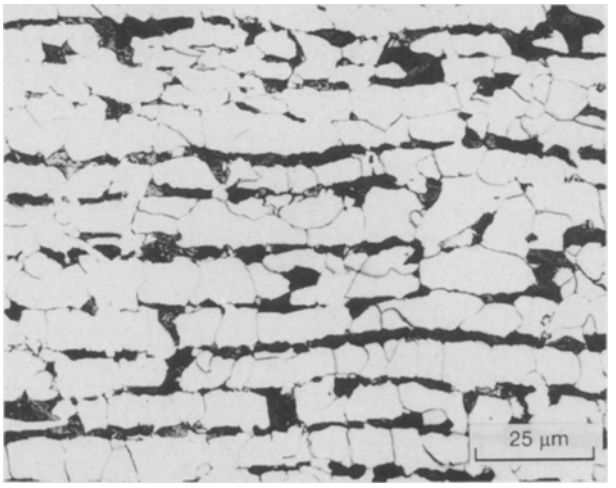

Figure 17 Effect of total finishing mill deformation on the final microstructure. Steel E1. Cooling rate = 3.5 °C s^{-1}.

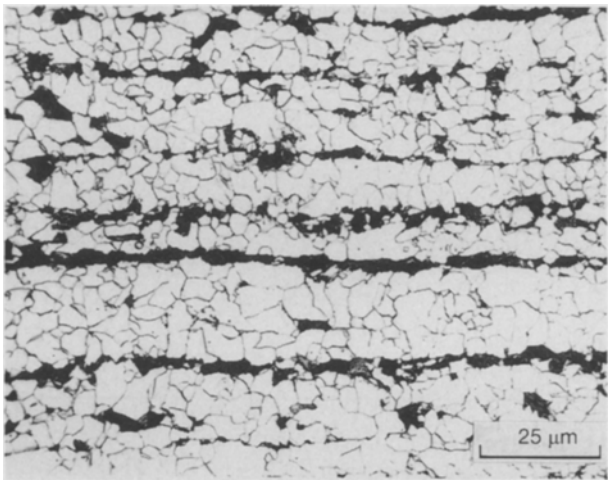

Figure 18 Effect of total finishing mill deformation on the final microstructure. Steel VE2. Cooling rate = 3.5 °C s^{-1}.

The results permit an evaluation of the influence of the vanadium on the recrystallized fraction and in particular on the activation energy, as well as its consequences for the hot rolling of this type of steel.

The second part of the study was given over to verifying the influence of the activation energy on the microstructural evolution of commercial steels E1 and VE2 when they are subjected to a simulated industrial finishing mill, a diagram of which is shown in Fig. 14. The interval of temperatures selected (825–785 °C) is lower than the recrystallization critical temperature of steel VE2, close to 900 °C, where very high activation energy values, of over 10^7 J mol^{-1}, were reached. At the end of the final pass, the specimens were quenched and prepared for etching in a saturated solution of picric acid, and the microstructures displayed in Figs 15 and 16 were obtained. Likewise, the simulation was performed and the specimens were cooled at a rate of 3.5 °C s^{-1}, measured between 780 °C and 500 °C, the microstructures of Figs 17 and 18 being obtained.

4. Discussion

An increase of the vanadium percentage hardly affects the austenitic grain size at the austenization temperatures (1230 °C), so vanadium cannot be considered an element that refines the austenitic grain in the temperature interval in which it is dissolved.

The $t_{0.5}$ values obtained are very similar in the three steels, if one compares those for the same temperature and strain, although the values of steel V2 are slightly lower, especially at a strain of 0.20.

Fairly similar values were obtained for the activation energy in the temperature interval in which it is constant (dissolved vanadium): 200 kJ mol^{-1}, 183 kJ mol^{-1} and 197 kJ mol^{-1} for steels V1, V2 and V3, respectively. Steel V2 had the lowest value, which will affect the parameter $t_{0.5}$. The results show that dissolved vanadium has no influence on the activation energy, in contrast to dissolved niobium, which does have a strong influence [10].

A comparison of the Q values measured experimentally and those calculated by Equation 3 shows that this equation may also be used to calculate the activation energy in these steels, and that the lower Q value in steel V2 is basically due to its higher carbon content. At the same time, the high level of accuracy of Equation 3, verified in a large number of steels, also shows that dissolved vanadium has no influence on Q.

The values obtained for the recrystallization critical temperature (Table II) demonstrate that this is not only a function of the vanadium percentage, but also of the amount of strain. While an increase in strain should accelerate the induced precipitation [15] and so favour inhibition of recrystallization, which would signify higher T_c values, the foregoing results show that the increase of defects (subgrains) caused by the increase in strain, which serve as recrystallization nuclei, has a greater effect and the result of both is that T_c drops as the strain rate rises. The curves of Fig. 13 demonstrate that the critical recrystallization temperatures fall between the dissolution temperatures of nitrides and carbides, signifying that the vanadium precipitates in these steels are basically of nitrides. This was to be expected if one takes into account their high nitrogen content (> 100 p.p.m.).

Consequently, Equation 3 may be used to calculate Q in vanadium microalloyed steels at temperatures at which there is no inhibition of recrystallization ($T > T_c$). When the temperature is below T_c, an additional term must be added to the energy calculated by Equation 3 in order to calculate the rapid increase of the activation energy. This term was calculated by regression, the following expression being obtained:

$$Q^* = 5.843 \times 10^{-38} V^{4.806} \varepsilon^{-3.9} \exp\left(\frac{700\,000}{RT}\right) \quad (6)$$

V being given in wt % × 10^3.

Equation 6 shows that at temperatures below T_c the activation energy depends on the temperature, strain and vanadium content. It is clear that the dependence on temperature is lower than that of niobium [10], signifying that once inhibition has commenced at T_c a certain drop in temperature leads to a greater inhibition of the recrystallization in Nb microalloyed steels than in V microalloyed steels. In other words, the austenite hardens more after the same strain. The equation proposed to calculate the activation energy of vanadium microalloyed steels will be:

$$Q_v = 83\,600 + 978\,000 \frac{(Mn + Si)^{0.537}}{C^{1.269}} + Q^* \quad (7)$$

where $Q^* = 0$ when $T > T_c$.

In the temperature intervals selected for simulating the finishing mill (Fig. 14) there is recrystallization inhibition in steel E1 because it is a typical C–Mn steel with an activation energy of 148 kJ mol^{-1}, calculated by Equation 3; yet there is a high level of inhibition in steel VE2 with high activation energy values (> 10^7 kJ mol^{-1}). For this reason, the microstructure of steel E1 (Fig. 15) has a much less deformed austenite than steel VE2 (Fig. 16), and while the austenite of E1 has experienced successive partial recrystallizations between passes, the austenite of VE2 has been continuously hardened. The stress–strain curves also demonstrate the strong hardening of steel VE2 compared to E1, but the microstructures are more illustrative.

It is known that an austenite hardened before the $\gamma \rightarrow \alpha$ transformation produces a smaller ferritic grain [16] and this is what is seen in the microstructures of Figs 17 and 18, obtained by cooling after simulation at a cooling rate of 3.5 °C s^{-1}. Thus, while steel E1 has an average ferritic grain size of 9 μm, steel VE2 has a grain size of approximately 4 μm. Finally, it must be pointed out that in practice, fine grain ferritic microstructures are desirable because, as is known [17, 18], they have better mechanical properties of yield strength, ultimate strength and transition temperature.

5. Conclusions

1. Dissolved vanadium only slightly affects the austenitic grain size, and cannot be considered an element that refines the grain size.
2. Dissolved vanadium has no influence on the activation energy, in contrast to niobium, which exerts a strong influence.
3. In the steels used, with nitrogen contents of over 100 p.p.m., recrystallization is inhibited as a result of the induced precipitation of nitrides.
4. Equation 3, or the first term of the second member of Equation 7, permits a very approximate calculation of the activation energy at temperatures above T_c in vanadium microalloyed steels with carbon contents of over 0.045%.
5. Equation 7 may be used to calculate the activation energy of vanadium microalloyed steels when the temperature is below T_c.
6. Vanadium microalloyed steels rolled at temperatures below T_c produce a strongly hardened austenite at the end of the rolling, making for a fine grain microstructure after the $\gamma \rightarrow \alpha$ transformation.
7. A certain drop of the temperature below the corresponding recrystallization critical temperatures, T_c, in Nb and V microalloyed steels leads to a greater hardening of the austenite in the former.

Acknowledgements

The authors are grateful for the financial support of the DGICYT of Spain (Project PB89-0022). Mancilla and Hernández's studies are sponsored by the University of Puebla and the National Univesity of Mexico, respectively.

References

1. C. M. SELLARS, in "Hot working and forming processes" (The Metals Society, London, 1980) p. 3.
2. *Idem. Mater. Sci. Eng.* **6** (1990) 1072.
3. P. CHOQUET, B. LAMBERTERIE. C. PERDRIX and H. BIAUSSER, in Proceedings of the 4th International Steel Rolling Conference, Deauville, France (IRSID, 1987) p. B.5.1.
4. P. CHOQUET, A. LE BON and C. PERDRIX, in Proceedings of the 7th International Conference on Strength of Metals and Alloys, Montreal, August 1985, edited by H. J. McQueen, J. B. Bailon, J. I. Dickson, J. J. Jonas and M. G. Akben, (Pergamon Press, Canada, 1985) p. 1025.
5. A. LAARASQUI and J. J. JONAS, *ISIJ Internat.* **31** (1991) 95.
6. H. L. ANDRADE, M. G. AKBEN and J. J. JONAS, *Met. Trans.*, **14A** (1983) 1967.
7. J. R. EVERETT, A. GITTINS, G. GLOVER and M. TOYAMA, in "Hot working and forming processes" (The Metals Society, London, 1980) p. 16.
8. S. YAMAMOTO, S. OUCHI and T. OSUKA, in Proceedings of the International Conference on Thermomechanical Processing of Microalloyed Austenite, Pittsburg, August 1981, edited by A. J. De Ardo, G. A. Ratz and P. J. Wray, (The Metallurgical Society of AIME, Pennsylvania, 1982) p. 613.
9. R. K. AMIN and F. B. PICKERING, *ibid.* p. 1.
10. S. F. MEDINA and P. FABREGUE, *J. Mater. Sci.* **26** (1991) 5427.
11. A. FAESSELL, *Rev. Métall., Cah. Inf. Tech.*, **4** (1976) 875.
12. B. MIGAUD, in "Hot working and forming processes" (The Metals Society, London, 1980) p. 67.
13. J. COUPRY, *Rev. Alum.* **5** (1978) 259.
14. K. NARITA, *Trans. ISIJ* **15** (1975) 145.
15. P. CHARLIER, in "Les aciers à dispersoïdes appliqués à la mécanique" (CETIM, Senlis, 1986) p. 21.
16. R. KASPAR, A. STREIBELBERGER and O. PAWELESKI, in Proceedings of the International Conference on Thermomechanical Processing of Microalloyed Austenite, Pittsburg, August 1981, edited by A. J. De Ardo, G. A. Ratz and P. J. Wray, (The Metallurgical Society of AIME, Pennsylvania, 1982) p. 555.
17. N. PETCH, *J. Iron Steel Inst.*, **174** (1953) 25.
18. T. GLADMAN, *Ironmaking Steelmaking* **16** (1989) 4.

Received 8 May 1992
and accepted 24 February 1993